J|A|C|S
ARTICLES
Published on Web 03/04/2003

Mechanism of Ketone and Alcohol Formations from Alkenes and Alkynes on the Head-to-head 2-Pyridonato-Bridged *cis*-Diammineplatinum(III) Dinuclear Complex

Nami Saeki,[†] Noriko Nakamura,[†] Takayuki Ishibashi,[†] Moritatsu Arime,[†] Hideo Sekiya,[†] Koji Ishihara,*[,†,‡] and Kazuko Matsumoto*[,†,§]

Contribution from the Department of Chemistry, School of Science and Engineering, Waseda University, Okubo, Shinjuku-ku, Tokyo 169-8555, Japan, Materials Research Laboratory for Bioscience and Photonics, Graduate School of Science and Engineering, Waseda University, Okubo, Shinjuku-ku, Tokyo 169-8555, Japan, and Advanced Research Institute for Science and Engineering, Waseda University, Okubo, Shinjuku-ku, Tokyo 169-8555, Japan

Received July 11, 2002; E-mail: ishi3719@waseda.jp

Abstract: Reactions of the head-to-head 2-pyridonato-bridged *cis*-diammineplatinum(III) dinuclear complex having nonequivalent two platinum atoms, $Pt(N_2O_2)$ and $Pt(N_4)$, with *p*-styrenesulfonate, 2-methyl-2-propene-1-sulfonate, 4-penten-1-ol, and 4-pentyn-1-ol were studied kinetically. Under the pseudo first-order reaction conditions that the concentration of the Pt^{III} dinuclear complex is much smaller than that of olefin, a consecutive basically four-step reaction was observed: the olefin π-coordinates preferentially to the $Pt(N_2O_2)$ in the first step (step 1), followed by the second π-coordination of another olefin molecule to the $Pt(N_4)$ (step 2). In the next step (step 3), the nucleophilic attack of water to the coordinated olefin triggers the $\pi-\sigma$ bond conversion on the $Pt(N_2O_2)$, and the second π-bonding olefin molecule on the $Pt(N_4)$ is released. Finally, reductive elimination occurs to the alkyl group on the $Pt(N_2O_2)$ to produce the alkyl compound (step 4). The first water substitution with olefin (step 1) occurs to the diaqua and aquahydroxo forms of the complex, whereas the second substitution (step 2) proceeds either on the coordinated OH^- on the $Pt(N_4)$ (path a) or on the coordinatively unsaturated five-coordinate intermediate of the $Pt(N_4)$ (path b), in addition to the common substitution of H_2O (path c). The reactions of *p*-styrenesulfonate and 2-methyl-2-propene-1-sulfonate proceed through paths b and c, whereas the reactions of 4-penten-1-ol and 4-pentyn-1-ol proceed through paths a and c. This difference reflects the difference of the trans effect and/or trans influence of the π-coordinated olefins on the $Pt(N_2O_2)$. The pentacoordinate state in path b is employed only by the sulfo-olefins, because these exert stronger trans effect. The steps 3 and 4 reflect the effect of the axial alkyl ligand (R) on the charge localization ($R-Pt^{IV}(N_2O_2)-Pt^{II}(N_4)$) and delocalization ($R-Pt^{III}(N_2O_2)-Pt^{III}(N_4)-OH_2$); when R is *p*-styrenesulfonate having an electron withdrawing group, the charge localization in the dimer is less pronounced and the water molecule on the $Pt(N_4)$ atom is retained ($R-Pt^{III}(N_2O_2)-Pt^{III}(N_4)-OH_2$) in the intermediate state. In both routes, the alkyl group undergoes nucleophilic attack of water, and the oxidized products are released via reductive elimination.

Introduction

The head-to-head (HH) Pt^{III} dinuclear complexes $[Pt_2(NH_3)_4(N\frown O)_2L_2]^{n+}$ ($N\frown O$ = amidate, L = NO_3^-, NO_2^-, H_2O, or Cl^-) derived from "platinum blues" have been found to act as catalysts for the oxidation of olefins to aldehydes, ketones, epoxides, and α,β-diols (Scheme 1).[1−4] In these reactions, it was suggested that olefins, which initially π-coordinates to the axial site of the Pt^{III} dinuclear complexes, are converted to the corresponding alkyl σ-complexes by nucleophilic attack of water to the coordinated olefins. Finally the oxidized products are released by reductive elimination. The α-carbon atom bound to the Pt atom receives the second nucleophilic attack of water

Scheme 1

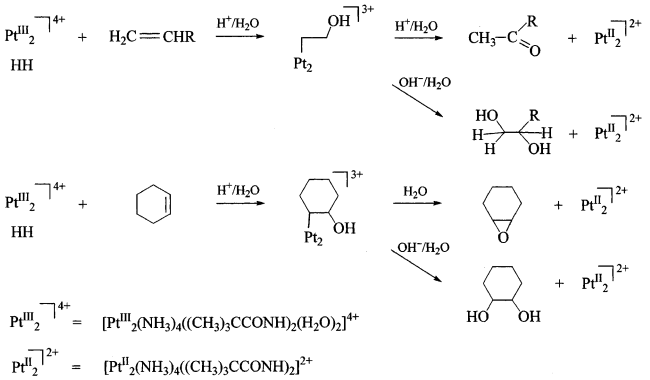

[†] Department of Chemistry.
[‡] Materials Research Laboratory.
[§] Advanced Research Institute for Science and Engineering.

(1) Matsumoto, K.; Mizuno, K.; Abe, T.; Kinoshita, J.; Shimura, H. *Chem. Lett.* **1994**, 1325.
(2) Matsumoto, K.; Nagai, Y.; Matsunami, J.; Mizuno, K.; Abe, T.; Somazawa, R.; Kinoshita, J.; Shimura, H. *J. Am. Chem. Soc.* **1998**, *120*, 2900.
(3) Lin, Y.-S.; Takeda, S.; Matsumoto, K. *Organometallics* **1999**, *18*, 4897.
(4) Matsumoto, K.; Sakai, K. *Adv. Inorg. Chem.* **1999**, *49*, 375.

10.1021/ja020953s CCC: $25.00

to release diols.[3,4] Several alkyl Pt^{III} dinuclear complexes have been synthesized by the reactions of $[Pt_2(NH_3)_4(pival-amidato)_2L_2]^{n+}$ with olefins such as 4-penten-1-ol and ethylene glycol vinyl ether, and their crystal structures have been determined by X-ray crystallography.[2] The two platinum atoms in the HH form are not equivalent: one is coordinated by two amidate oxygen and two ammine nitrogen atoms ($Pt(N_2O_2)$), and the other is coordinated by two ammine nitrogen and two amidate nitrogen atoms ($Pt(N_4)$). The alkyl groups in the alkyl Pt^{III} complexes mentioned above and the halide ions in the monohalo complexes always bind to the $Pt(N_2O_2)$, which means that the $Pt(N_2O_2)$ atom would have higher reactivity to olefins and halides. Thus, it seems probable that the $Pt(N_2O_2)$ plays an important role in the catalytic reactions of the dinuclear Pt^{III} complexes. This is an important feature, especially if we think of the novel dinuclear structure having a $Pt^{III}-Pt^{III}$ bond, through which the actual electron density of the two platinum atoms is adjusted, depending on the axial ligand.[2]

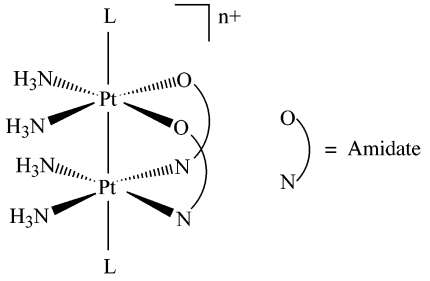

Head-to-Head
(HH)

It is well-known that Pt(II) complexes react with olefins to form π-complexes such as Zeise's salt $K[PtCl_3(C_2H_4)]\cdot H_2O$,[5] and their reactivities are also known.[6−11] In contrast, Pt(IV) usually does not react with olefins, and only an exceptional Pt(IV) complex is known to react with olefin. The reactivity of the complex is not known.[12,13] The role of Pt^{II}-olefin and Pt^{IV}-alkyl intermediates are emphasized as the key compounds to understand the mechanistic aspects of the oxidative functionalization of ethane and ethanol by Pt(II) salts in aqueous medium.[14−16] However, no definite conclusion has been drawn about the mechanism, and the kinetics data are reported only to the ethene exchange kinetics of Pt(II) chloro ethene π-complexes.[7,17]

As for Pt(III) complexes, the knowledge of the reactivity is much more limited compared to Pt(II) and Pt(IV).[18−20] However, our recent study revealed that Pt^{III} dinuclear complexes catalyze olefin oxidation to a certain extent, and to our surprise, β-hydroxyalkyl-Pt^{III} dinuclear complexes were isolated and the crystal structures were solved.[2,3] These complexes correspond to the intermediates of the olefin oxidation on Pt(III), and are very significant considering the fact that analogous hydroxyalkyl-Pt^{II} complexes cannot be isolated.

In this paper, we report the first kinetic and mechanistic study on the reactions of the Pt^{III} dinuclear complex $[Pt_2(NH_3)_4(\alpha\text{-pyridonato})_2(H_2O)_2]^{4+}$ with olefins and alkyne. The study is focused on how the dinuclear Pt^{III} complex utilizes its Pt(II) and Pt(IV) character at each step of the reaction to stabilize the alkyl Pt^{III} complexes. The present study clearly shows the conversion of the π-coordinated olefin-Pt^{III} to σ-alkyl-Pt^{III} on nucleophilic attack of water. The kinetic data are significant considering the relevance of the reaction to Wacker process.

Experimental Section

Reagents. *cis*-$[Pt(NH_3)_2Cl_2]$ was prepared from $K_2[PtCl_4]$ (Tanaka Kikinzoku Kogyo K. K., Tokyo) according to the Dhara's method.[21] Reagent grade 2-pyridone (Kanto Chemical Co. Inc., Tokyo) was recrystallized once from benzene. Sodium p-styrenesulfonate (Tokyo Chemical Industry Co. Ltd.) and 5-Norbornene-2,2-dimethanol (Aldrich) were used without further purification. 4-Penten-1-ol (Tokyo Chemical Industry Co. Ltd.) and 4-pentyn-1-ol (Aldrich) were purified once by vacuum distillation. Sodium 2-methyl-2-propene-1-sulfonate (Aldrich) was recrystallized once from water. Perchloric acid (60% UGR for trace analysis, Kanto) was used as received. Sodium perchlorate was prepared and purified according to the literature.[22] Head-to-head $[(H_2O)(NH_3)_2Pt(\mu\text{-}C_5H_4NO)_2Pt(NH_3)_2(NO_3)](NO_3)_3\cdot 2H_2O$ (HH complex) was prepared according to the literature.[23]

Measurements. Ionic strength was maintained at 2.00 M with perchloric acid and sodium perchlorate. All the sample solutions were prepared by using twice distilled water just before measurement. Spectrophotometric measurements were performed with a rapid-scan/stopped-flow spectrophotometer USP-500 (Unisoku Scientific Instruments, Osaka) and spectrophotometers UV-160A (Shimadzu, Kyoto), UV-2200 (Shimadzu), and UV-2400 (Shimadzu). Rate constants were measured by monitoring the absorbance change at 350 nm for the reaction of the HH complex with sodium *p*-styrenesulfonate, 265 nm for the reactions with 4-penten-1-ol and sodium 2-methyl-2-propenesulfonate, and 268 nm for the reaction with 4-pentyn-1-ol, as a function of time after mixing the solutions of the complex and the ligands. The solution of 4-penten-1-ol was prepared with 10% (v/v) ethanol because of the insolubility of the ligand in water, whereas a 100% aqueous solution was prepared for the HH complex, since the complex is slowly reduced by alcohols. Therefore, the final reaction solution contained 5% ethanol after mixing. Under the conditions that the concentrations of the ligands (C_L) are in large excess over that of the complex (C_{HH}), the reaction was found to consist of several consecutive first-order steps. Kinetic measurements for the *p*-styrenesulfonate system were performed also under the conditions, $C_{HH} \gg C_L$.

The absorbance change for the 2-methyl-2-propene-1-sulfonate system was similar to that for the *p*-styrenesulfonate, i.e., a four-step reaction was observed, but the absorbance changes for the steps 1 and 3 were too small to calculate the reliable rate constants. For the 4-penten-1-ol and 4-pentyn-1-ol systems, the initial two steps were succeeded by a very slow reaction which could not be analyzed

(5) Zeise, W. C. *Magn. Pharm.* **1830**, *35*, 105.
(6) Cramer, R. *Inorg. Chem.* **1965**, *4*, 445.
(7) Olsson, A.; Kofod, P. *Inorg. Chem.* **1992**, *31*, 183.
(8) Leden, I.; Chatt, J. *J. Chem. Soc.* **1955**, 2936.
(9) Lokken, S. J.; Martin, D. S. *Inorg. Chem.* **1963**, *2*, 562.
(10) McMane, D. G.; Martin, D. S., Jr. *Inorg. Chem.* **1968**, *7*, 1169.
(11) Chatt, J.; Williams, A. A. *J. Chem. Soc.* **1951**, 3061.
(12) Howard, W. A.; Bergman, R. G. *Polyhedron* **1998**, *17*, 803.
(13) Persons, E. J.; Larsen, R. D.; Jennings, P. W. *J. Am. Chem. Soc.* **1985**, *107*, 1793.
(14) Hutson, A. C.; Lin, M.; Basickes, N.; Sen, A. *J. Organomet. Chem.* **1995**, *504*, 69.
(15) Fanizzi, F. P.; Intini, F. P.; Maresca, L.; Natile, G.; Lanfranchi, M.; Tiripicchio, A. *J. Chem. Soc., Dalton Trans.* **1991**, 1007.
(16) Fanizzi, F. P.; Maresca, L.; Pacifico, C.; Natile, G.; Lanfranchi, M.; Tiripicchio, A. *Eur. J. Inorg. Chem.* **1999**, 1351.
(17) (a) Plutino, M. R.; Otto, S.; Roodt, A.; Elding, L. I. *Inorg. Chem.* **1999**, *38*, 1233. (b) Otto, S.; Elding, L. I. *J. Chem. Soc., Dalton Trans.* **2002**, 2354.
(18) Saeki, N.; Hirano, Y.; Sasamoto, Y.; Sato, I.; Toshida, T.; Ito, S.; Nakamura, N.; Ishihara, K.; Matsumoto, K. *Bull. Chem. Soc. Jpn.* **2001**, *74*, 861.
(19) Saeki, N.; Hirano, Y.; Sasamoto, Y.; Sato, I.; Toshida, T.; Ito, S.; Nakamura, N.; Ishihara, K.; Matsumoto, K. *Eur. J. Inorg. Chem.* **2001**, *2001*, 2081.
(20) El-Mehdawi, R.; Bryan, S. A.; Roundhill, D. M. *J. Am. Chem. Soc.* **1985**, *107*, 6282.
(21) Dhara, S. C. *Indian J. Chem.* **1970**, *8*, 193.
(22) Funahashi, S.; Haraguchi, K.; Tanaka, M. *Inorg. Chem.* **1977**, *16*, 1349.
(23) Hollis, L. S.; Lippard, S. J. *Inorg. Chem.* **1983**, *22*, 2605.

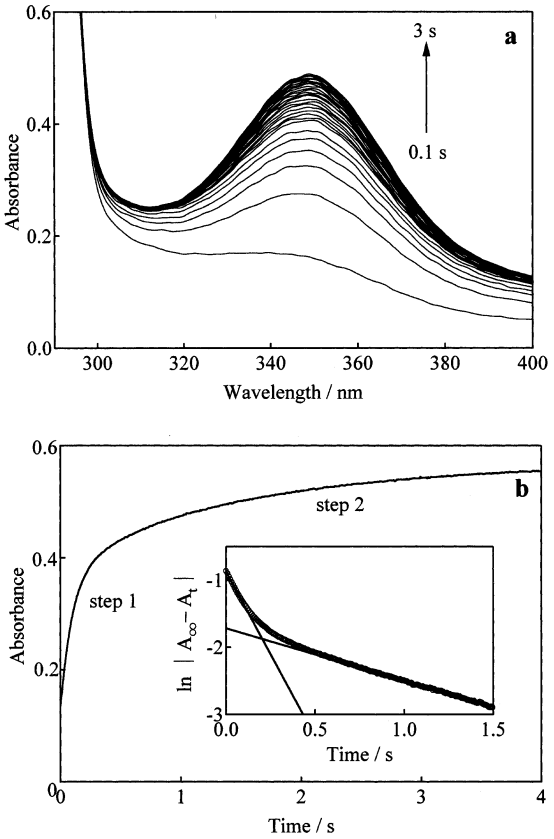

Figure 1. (a) Change of the UV−vis spectrum for steps 1 and 2 in Scheme 3, taken every 100 ms at $I = 2.0$ M and 25 °C. $C_{HH} = 2 \times 10^{-5}$ M, $C_L = 2.42 \times 10^{-3}$ M, and $[H^+] = 0.0318$ M. (b) The absorbance change with time at 350 nm in Figure 1a. The inset shows the semilog plot of the data.

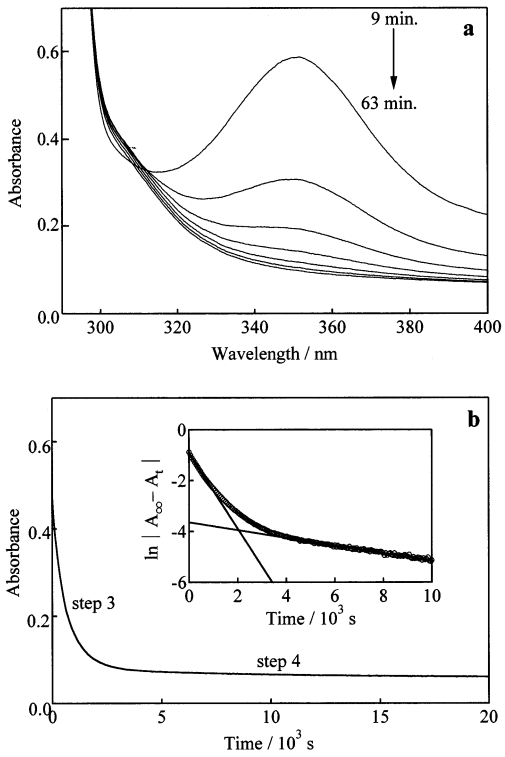

Figure 2. (a) Change of the UV−vis spectrum for steps 3 and 4 in Scheme 3, taken every 9 min at $I = 2.0$ M and 25 °C. $C_{HH} = 2 \times 10^{-5}$ M, $C_L = 2.50 \times 10^{-3}$ M, and $[H^+] = 0.0318$ M. (b) The absorbance change with time at 350 nm in Figure 1b. The inset shows the semilog plot of the data.

kinetically. The reaction with 5-norbornene-2,2-dimethanol was also studied, but the ^{1}H NMR spectra were too complicated to identify the product, and so no further analysis was performed.

The ^{1}H NMR spectra were recorded on a JEOL Lambda 270 spectrometer. The chemical-shift was referenced to TMA (tetramethylammonium perchlorate, 3.190 ppm to TMS).

Results and Discussion

Reaction with Sodium *p*-Styrenesulfonate. The reaction with sodium *p*-styrenesulfonate gives *p*-sulfonatoacetophenone (*p*-acetylbenzenesulfonate) and the Pt(II) dimer complex as shown in eq 1. Changes in UV−vis absorption spectra with time under the pseudo first-order condition, $C_{HH} \ll C_L$, are shown in Figures 1a and 2a. Figures 1b and 2b show the time course change in absorbance at 350 nm in Figures 1a and 2a,

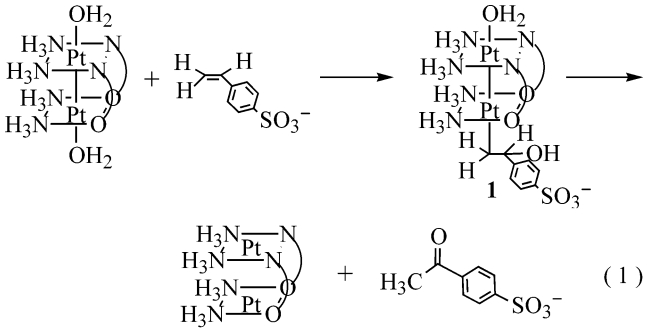

(1)

respectively. Both indicate that the present reaction consists of four steps; the fastest step (step 1), two intermediate steps (steps 2 and 3), and the slowest step (step 4). The insets in Figures 1b and 2b show that the reaction consists of four consecutive first-order reactions. The pseudo first-order rate constants, k_{obs1}, k_{obs2}, and k_{obs3} for steps 1−3, respectively, were dependent on the excess ligand concentration, which suggests that steps 1−3 are intermolecular processes, and k_{obs1} and k_{obs3} were also dependent on $[H^+]$, but k_{obs2} was not, as shown in Figure 3. It is noteworthy that k_{obs3} decreases drastically with increasing C_L. On the other hand, the k_{obs4} was not dependent either on C_L or $[H^+]$ (Figure 3).

We reported previously the axial ligand substitutions with halides on the same HH complex as used in this study, and proposed the mechanisms depicted in Scheme 2 for the observed consecutive two-step reactions.[18] In this scheme, the first ligand substitution reaction with halide ion occurs to the $Pt(N_2O_2)$ of the HH complex (the left and upper step in Scheme 2), and the first deprotonation of the aqua ligand occurs to the $H_2O-Pt(N_4)$ exclusively (the left equilibrium in Scheme 2), and the second substitution takes place on the $Pt(N_4)$ (the right and upper steps in Scheme 2). The reactive species having an unsaturated coordination site is postulated for the second ligand substitution reaction (Scheme 2). The rate constants of steps 1 and 2 for the present *p*-styrenesulfonate system (Figure 3) varied with C_L and $[H^+]$ in the same way as those for the first (k_{obs1}) and second (k_{obs2}) halide substitutions on the HH complex, respectively. The close similarity between the present system and the halide system led us to consider similar reaction steps in the present system (see steps 1 and 2 in Scheme 3). In Scheme 3, the first π-coordination of the olefin occurs to the $Pt(N_2O_2)$ (step 1) and

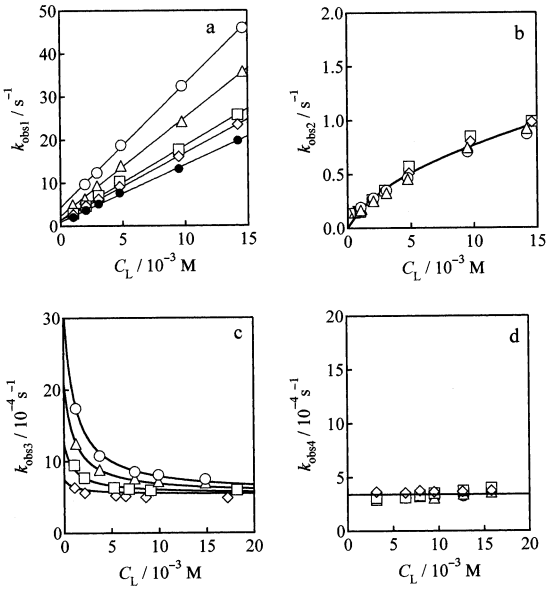

Figure 3. Dependence of the observed rate constants on C_L for the reaction of the HH dimer with *p*-styrenesulfonate at $I = 2.0$ M. (a) For step 1, at 25 °C and [H$^+$]/M = 0.0101 (○), 0.0201 (△). 0.121 (□), 0.201 (◇), and 0.403 (●). (b) For step 2, at 25 °C and [H$^+$]/M = 0.201 (○), 0.403 (△). 0.805 (□), and 1.21 (◇). (c) For step 3, at 25 °C and [H$^+$]/M = 0.03181 (○), 0.153 (△). 0.403 (□), and 0.805 (◇). (d) For step 4, at 35 °C and [H$^+$]/M = 0.206 (○), 0.411 (△). 0.822 (□), and 1.64 (◇).

Scheme 2

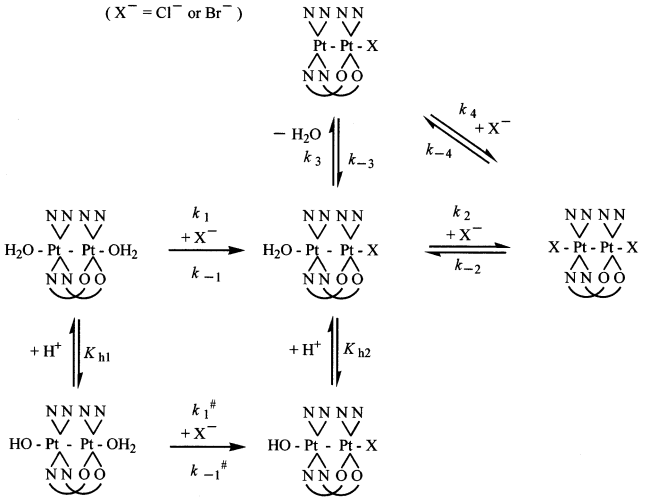

the second π-coordination of the olefin occurs to the Pt(N_4) (step 2).

The experimental data in Figure 3a give eq 2 for k_{obs1}, and eq 3 is derived from the reaction paths in Scheme 3

$$k_{obs1} = k_{f1}C_L + k_{d1} \tag{2}$$

$$k_{obs1} = \frac{k_1 + \dfrac{k_1^{\#}K_{h1}}{[H^+]}}{1 + \dfrac{K_{h1}}{[H^+]}}[L] + \frac{k_{-1} + \dfrac{k_{-1}^{\#}K_{h2}}{[H^+]}}{1 + \dfrac{K_{h2}}{[H^+]}} \tag{3}$$

Equations 4 and 5 are obtained from eqs 2 and 3, under the present condition $C_{HH} \ll C_L$. The values k_{f1} and k_{d1} are the rate

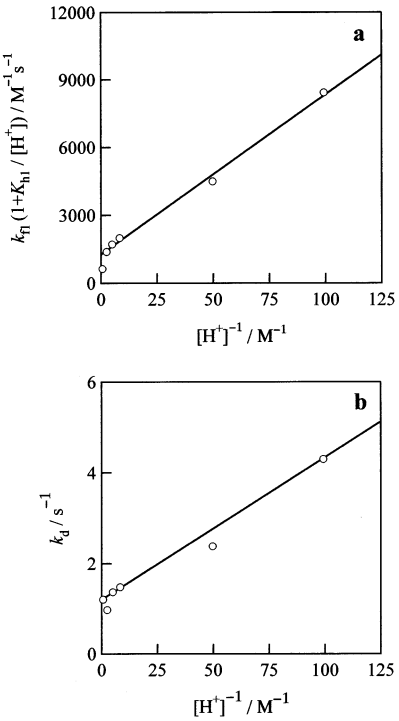

Figure 4. Dependence of k_{f1} (a) and k_{d1} (b) (for step 1 in Figure 3a) on [H$^+$] for the reaction with *p*-styrenesulfonate.

constants of the forward and the reverse reactions of step 1 in Scheme 3, respectively

$$k_{f1} = \frac{k_1 + \dfrac{k_1^{\#}K_{h1}}{[H^+]}}{1 + \dfrac{K_{h1}}{[H^+]}} \tag{4}$$

$$k_{d1} = \frac{k_{-1} + \dfrac{k_{-1}^{\#}K_{h2}}{[H^+]}}{1 + \dfrac{K_{h2}}{[H^+]}} \doteqdot k_{-1} + \frac{k_{-1}^{\#}K_{h2}}{[H^+]} \tag{5}$$

The pH dependencies of k_{f1} and k_{d1} are shown in Figure 4. In the denominator of eq 5, $K_{h2}/[H^+]$ is negligible compared to unity under the present conditions, since the plot in Figure 4b is linear within the experimental errors.

On the other hand, k_{obs2} for step 2 in Scheme 3 is expressed with eq 6, when the steady-state approximation is applied to the coordinatively unsaturated complex (step 2 in Scheme 3) as was the halide case[18]

$$k_{obs2} = k_2[L] + \frac{k_3[L]}{[L] + \dfrac{k_{-3}}{k_4}} \tag{6}$$

The rate constants for steps 1 and 2 in this system are comparable to those in the halide system as shown in Table 1, which supports the validity of the proposed mechanism in Scheme 3.

Scheme 3. Reaction Mechanism for the Reaction of the HH Dimer with Sodium *p*-Styrenesulfonate

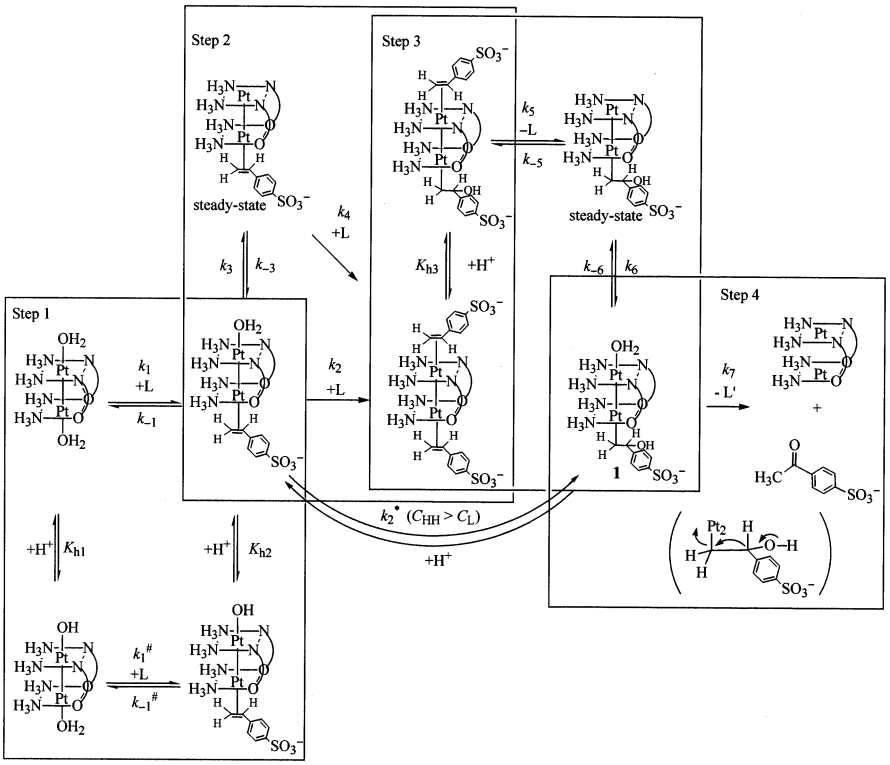

Table 1. Rate and Equilibrium Constants for the Reactions of the HH 2-Pyridonato-Bridged Diammineplatinum(III) Dinuclear Complex with Sodium *p*-Styrenesulfonate, Sodium 2-Methyl-2-propene-1-sulfonate, 4-Penten-1-ol, 4-Pentyn-1-ol, and Sodium Halides at 25 °C and $I = 2.0$ M

	p-styrenesulfonate[a]	2-methyl-2-propene-1-sulfonate	4-penten-1-ol	4-pentyn-1-ol	Cl^- [a]	Br^- [a]
step 1	$k_1 = 1.3 \times 10^3$ M^{-1} s^{-1}				$k_1 = 3.1 \times 10^3$ M^{-1} s^{-1}	$k_1 = 7.2 \times 10^3$ M^{-1} s^{-1}
	$k_1^\# = 4.4 \times 10^3$ M^{-1} s^{-1}				$k_1^\# = 4.6 \times 10^5$ M^{-1} s^{-1}	$k_1^\# = 2.4 \times 10^5$ M^{-1} s^{-1}
	$k_{-1} = 0.90$ s^{-1}					
	$k_{-1}^\# K_{h2} = 8.9 \times 10^{-2}$ M s^{-1}					
	$K_{h2} = 3.8 \times 10^{-4}$ M					
step 2	$k_2 = 31 \pm 3$ M^{-1} s^{-1}	$k_2 = 26 \pm 9$ M^{-1} s^{-1}	$k_2 = 29$ M^{-1} s^{-1}	$k_2 = 29$ M^{-1} s^{-1}	$k_2 = 550 \pm 10$ M^{-1} s^{-1}	$k_2 = 450 \pm 36$ M^{-1} s^{-1}
	$k_3 = 0.64 \pm 0.06$ s^{-1}	$k_3 = 0.23 \pm 0.12$ s^{-1}	$k_2^\# K_{h2} = 3.9 \times 10^2$ s^{-1}	$k_2^\# K_{h2} = 1.2 \times 10^2$ s^{-1}	$k_3 = 3.1 \pm 0.3$ s^{-1}	$k_3 = 4.4 \pm 0.8$ s^{-1}
	$k_{-3}/k_4 = 4.0 \times 10^{-3}$ M	$k_{-3}/k_4 = (2.2 \pm 1.4) \times 10^{-3}$ M	$K_{h2} = 6.3 \times 10^{-3}$ M	$K_{h2} = 1.0 \times 10^{-2}$ M	$k_{-3}/k_4 = 3.7 \times 10^{-3}$ M	$k_{-3}/k_4 = 3.7 \times 10^{-3}$ M
			$k_2^\# = 6.2 \times 10^4$ M^{-1} s^{-1}	$k_2^\# = 1.2 \times 10^4$ M^{-1} s^{-1}		
step 3	$k_5 K_{h3} = 7.1 \times 10^{-4}$ M s^{-1}		$k_{-3} = 44$ M^{-1} s^{-1}	$k_{-3} = 0.070$ M^{-1} s^{-1}		
	$K_{h3} = 0.21$ M	-	$k_3 K_{h3} = 8.4 \times 10^{-3}$ Ms^{-1}	$k_3 K K_{h3} = 7.3 \times 10^{-3}$ Ms^{-1}	-	-
	$k_{-5}k_{-6}/k_6 = 0.39$ M^{-1} s^{-1}		$K_{h3} = 7.2 \times 10^{-3}$ M	$K K_{h3} + K_{h3} = 2.4 \times 10^{-3}$ M		
	$k_{-5}/k_6 = 7.5 \times 10^2$ M^{-1}					
	$k_5 = 3.7 \times 10^{-3}$ s^{-1}					
	$k_{-6} = 5.4 \times 10^{-4}$ s^{-1}					
step 4	$k_7 = 3.4 \times 10^{-3}$ s^{-1} [b]	$k_6 = 1.0 \times 10^{-4}$ s^{-1}	-	-	-	-

[a] $K_{h1} = 0.0195$ M (25 °C, $I = 2.0$ M) was used.[18] [b] At 35 °C.

Figure 5 shows the change of the ^{1}H NMR spectrum after the reaction was started under the condition, $C_{HH} < C_L$. At $t =$ 40 min, only the peaks corresponding to the σ-complex (**1**) were observed, whereas at $t = 46$ h, the peaks of the free ketone and HH $[Pt^{II}_2(NH_3)_4(\alpha\text{-pyridonato})_2]^{2+}$ were observed. The latter is the reduction product of the HH $[Pt^{III}_2(NH_3)_4(\alpha\text{-pyridonato})_2]^{4+}$. The formation of the σ-complex was confirmed by the ^{1}H NMR spectrum because the isolation of the σ-complex was unsuccessful. The coupling constants among H_a, H_b, and H_c, and the chemical shifts depicted in Figure SI-1 are $^2J(H_a - H_b) = 9$ Hz, $^3J(H_b - H_c) = 9$ Hz, and $^3J(H_a - H_c) < 2$ Hz, and $\delta(H_a) = 4.67$ ppm, $\delta(H_b) = 4.24$ ppm, and $\delta(H_c) = 5.04$ ppm, which confirm the formation of the σ-complex. The peak height change with time in Figure 5 reasonably corresponds to steps 3 and 4 in Figure 2, i.e., the σ-complex **1** is formed at step 3, and reduction of the Pt^{III} dinuclear complex to the Pt^{II} dinuclear complex and oxidation of the alcoholyl group in the σ-complex to free ketone takes place at step 4.

The observed rate constant for step 3, k_{obs3}, varied with $[H^+]$ and decreased drastically with increasing C_L (Figure 3c). The π-bond $\rightleftarrows$ σ-bond conversion must be involved in step 3, because no other reaction is expected to release proton. The $\pi-\sigma$ conversion seems to take place on the $Pt(N_2O_2)$, because all the alkyl groups in the alkyl-$Pt(III)_2$ complexes reported so far are ligated to the $Pt(N_2O_2)$.[2,24,25] Our previous ^{195}Pt NMR studies of the alkyl-$Pt(III)_2$ complexes show that the electrons in the Pt−Pt bonds are localized and the real electronic state is close to $Pt^{II}(N_4)-Pt^{IV}(N_2O_2)$.[24] Therefore, the olefin on the Pt-

(24) Matsumoto, K.; Matsunami, J.; Mizuno, K.; Uemura, H. *J. Am. Chem. Soc.* **1996**, *118*, 8959.
(25) Sakai, K.; Tanaka, Y.; Tsuchiya, Y.; Hirata, K.; Tsubomura, T.; Iijima, S.; Bhattacharjee, A. *J. Am. Chem. Soc.* **1998**, *120*, 8366.

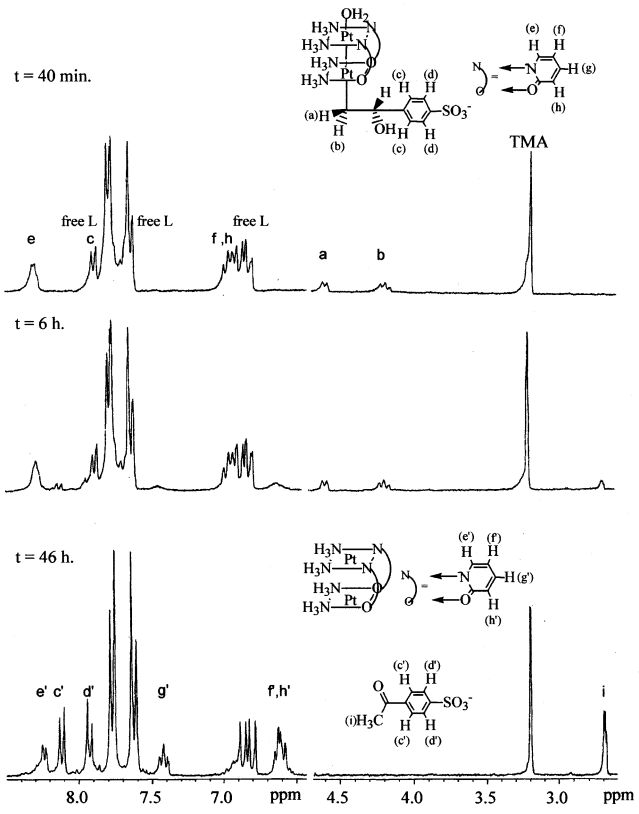

Figure 5. Change of the ^{1}H NMR spectrum with time at 5 °C, after mixing the HH dimer and the *p*-styrenesulfonate solutions. $C_{HH} = 4.3 \times 10^{-3}$ M, $C_L = 2.2 \times 10^{-2}$ M, and $[DClO_4] = 0.5$ M. The chemical shift was referenced to TMA (tetramethylammonium perchlorate).

(N_2O_2) is more easily subjected to nucleophilic attack by H_2O. If step 3 involves a simple substitution reaction preceded by the preequilibrium as shown in eq 7, which is actually the case for the 4-penten-1-ol system mentioned later, k_{obs3} is given by eq 8. However, eq 8 is inconsistent with the experimental result.

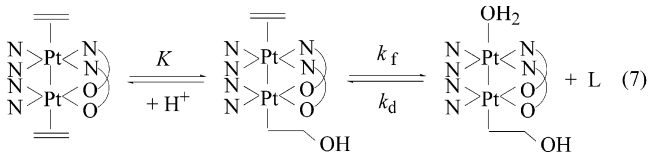

(7)

$$k_{obs3} = \frac{k_f K}{[H^+] + K} + k_d[L] \tag{8}$$

The reactive intermediate having the unsaturated coordination site at step 3 in Scheme 3 is necessary to explain the drastic decrease of k_{obs3} with increasing C_L. Equation 9 is

$$k_{obs3} = \frac{\dfrac{k_5 K_{h3}}{[H^+] + K_{h3}} + \dfrac{k_{-5}k_{-6}[L]}{k_6}}{\dfrac{k_{-5}[L]}{k_6} + 1} \tag{9}$$

derived when the steady-state approximation is applied to the intermediate at step 3 in Scheme 3. This equation agrees excellently with the experimental data as shown in Figure 3c.

The k_{obs4} is independent of both C_L and $[H^+]$ as shown in Figure 3d. This fact coincides with step 4 in Scheme 3, and therefore eq 10 holds. At step 4, the intramolecular reaction proceeds and the Pt^{III} complex is reduced to the HH Pt^{II} dinuclear complex to produce the ketone

$$k_{obs4} = k_7 \tag{10}$$

The best-fit curves in Figure 3 that were drawn by applying a nonlinear least-squares fitting of eqs 3, 6, 9, and 10 to the experimental data, agree well with the experimental results. All the rate constants in these equations were calculated by using $K_{h1} = 1.95 \times 10^{-2}$ M (25 °C, $I = 2.0$ M) determined previously,[14] and are tabulated in Table 1.

Scheme 4. Reaction Mechanism for the Reaction of the HH Dimer with Sodium 2-Methyl-2-propene-1-sulfonate

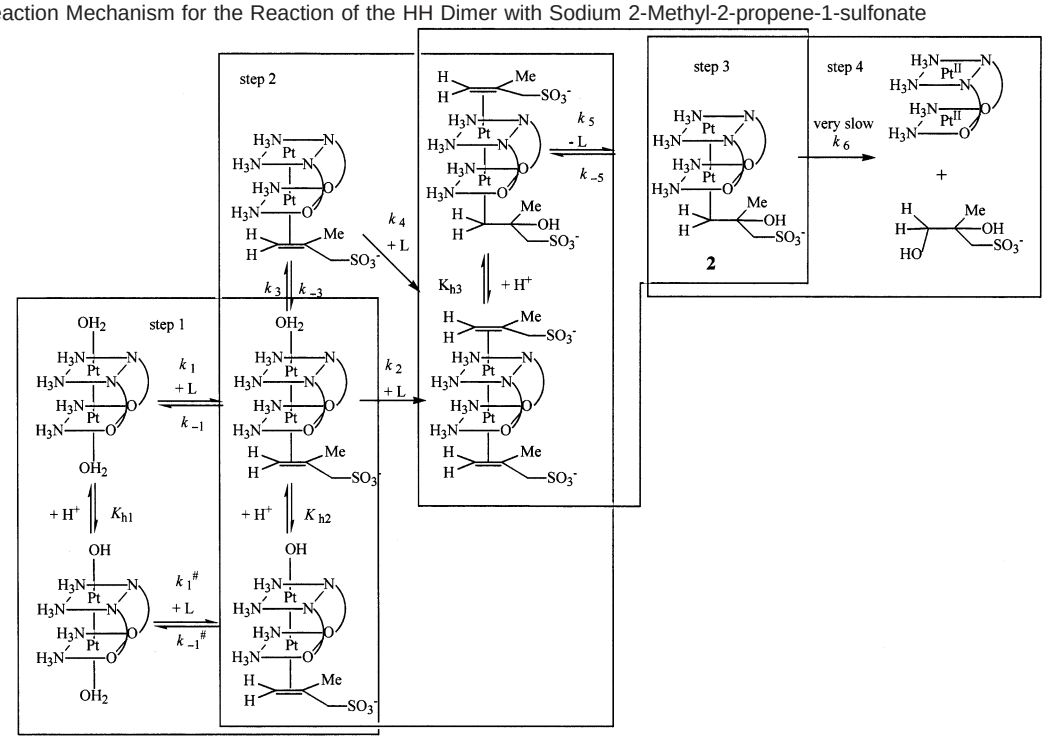

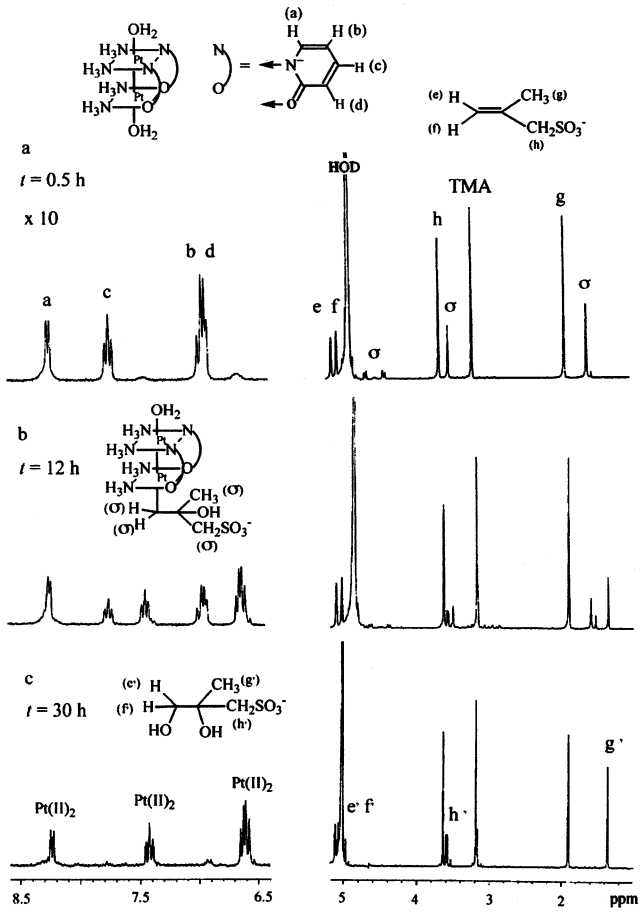

Figure 6. Change of the ^{1}H NMR spectrum with time at room temperature after mixing the HH dimer and the 2-methyl-2-propene-1-sulfonate solutions. $C_L/C_{HH} = 5$ and $[DClO_4] = 0.03$ M. (a) At $t = 0.5$ h, (b) at $t = 12$ h, and (c) at $t = 30$ h. The spectrum at lower field is 10-fold magnified.

There seems to be another reaction path (k_2* path in Scheme 3) which is not through the di-π-coordinated complex, under the condition $C_L \ll C_{Pt2}$, since the formation of the σ-complex and the ketone was also observed in the ^{1}H NMR spectrum under such condition, and the UV−vis spectral change was very slow, showing the decrease of the mono-π-complex.

Reaction with Sodium 2-Methyl-2-propene-1-sulfonate. The reaction with 2-methyl-2-propene-1-sulfonate gave 2-methyl-2,3-propanediol-1-sulfonate as the final product (eq 11). The reason for not having the axial ligand in the intermediate complex (**2**) in eq 11 is given later in the section of "Effect of the Axial Ligands on the Kinetics".

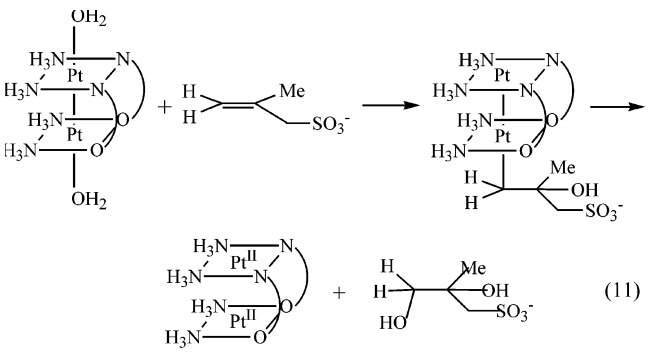

(11)

The absorbance change for this system was similar to that of the *p*-styrenesulfonate system, showing a similar four-step reaction, but the absorbance change for steps 1 and 3 was too small to calculate the reliable rate constants, as shown in Figure SI-2. Figure 6 shows the time dependent ^{1}H NMR spectra of the system. The spectrum at $t = 0.5$ h mainly consists of the peaks of the free ligand and the σ-complex **2**. The peaks of the σ-complex diminished with time, while the new peaks of the 1,2-diol and the HH Pt^{II} dinuclear complex increased at the same time. As Figure 7a shows, k_{obs2} was invariable with $[H^+]$ within the experimental error, but increased along a curved line with increasing C_L, which is very similar to step 2 in the *p*-styrenesulfonate system. The k_{obs3} clearly increased with C_L, whereas the pH dependence of k_{obs3} was not obvious (Figure 7b), since the values are less reliable due to the small spectral change mentioned above. This fact is a striking contrast to step 3 in the *p*-styrenesulfonate system (Figure 3c). On the other hand, k_{obs4} for step 4 did not depend on either $[H^+]$ or C_L (Figure 7c), which is the same as for the *p*-styrenesulfonate system. The four-step reaction mechanism of 2-methyl-2-propene-1-sulfonate can be constructed as in Scheme 4, on the basis of Scheme 3. Equations 6 and 12 can be derived for steps 2 and 4 in Scheme 4

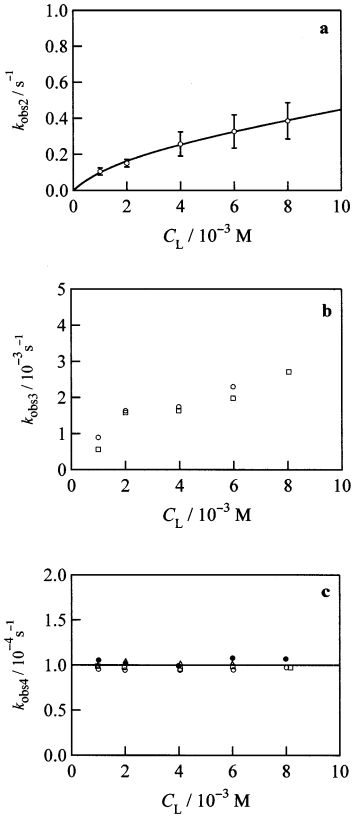

Figure 7. Dependence of the observed rate constants on C_L for the reaction of the HH dimer with 2-methyl-2-propene-1-sulfonate at $I = 2.0$ M and 25 °C. (a) For step 2, $[H^+] = 0.6-1.4$ M. (b) For step 3, $[H^+]/M = 0.617$ (□) and 0.411 (○). (c) For step 4, $[H^+]/M = 0.0514$ (○), 0.103 (□), 0.206 (△), and 0.411 (●).

$$k_{obs4} = k_6 \tag{12}$$

Reaction with 4-Penten-1-ol. The reaction with 4-penten-1-ol gave the tetrahydrofurfuryl complex as shown in eq 13.

A two-step reaction was observed under the pseudo first-order conditions ($C_{HH} \ll C_L$) as shown in Figure SI-3. The faster step and the slower step were exactly first order, and no further

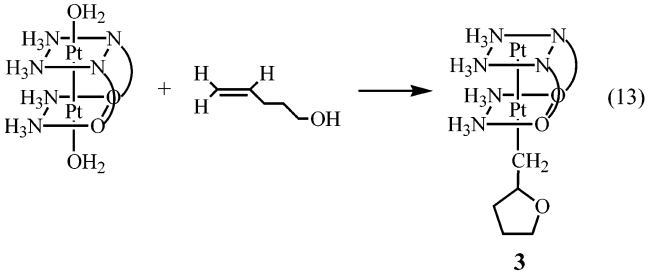

(13)

3

reaction was observed for at least a couple of hours, but extremely slow and slight spectral change was observed in several hours, which corresponds to the decomposition of the σ-complex **3**. Figure 8a shows the ^{1}H NMR spectrum measured at $t = 30$ min after the reaction was started. Free 4-penten-1-ol, the bridging pyridonato ligands, and the tetrahydrofurfuryl protons of the σ-complex, and some unknown compound(s) were observed. The structure of the σ-complex would be analogous to that of the previously reported pivalamidato-bridged analogue whose structure was elucidated by X-ray crystallography.[2] As the reaction proceeded, the σ-complex precipitated as fine crystals, whose elemental analysis agreed with the expected structure (Anal. Calcd for $[Pt_2(NH_3)_4(C_5H_4NO)_2(C_5H_9O)](NO_3)_2(ClO_4)$: C, 18.86; H, 3.06; N, 11.73. Found: C, 18.63; H, 2.59; N, 11.40.). The ^{1}H NMR spectra of the σ-complex precipitate dissolved in 1 M $DClO_4$ and measured at $t = 45$ min and 5 h after dissolution are depicted in Figure 8b and 8c, respectively, and show that the σ-complex changes very slowly to unknown product(s), and that no Pt^{II} dinuclear complex is produced [the bridging α-pyridonato peaks of the

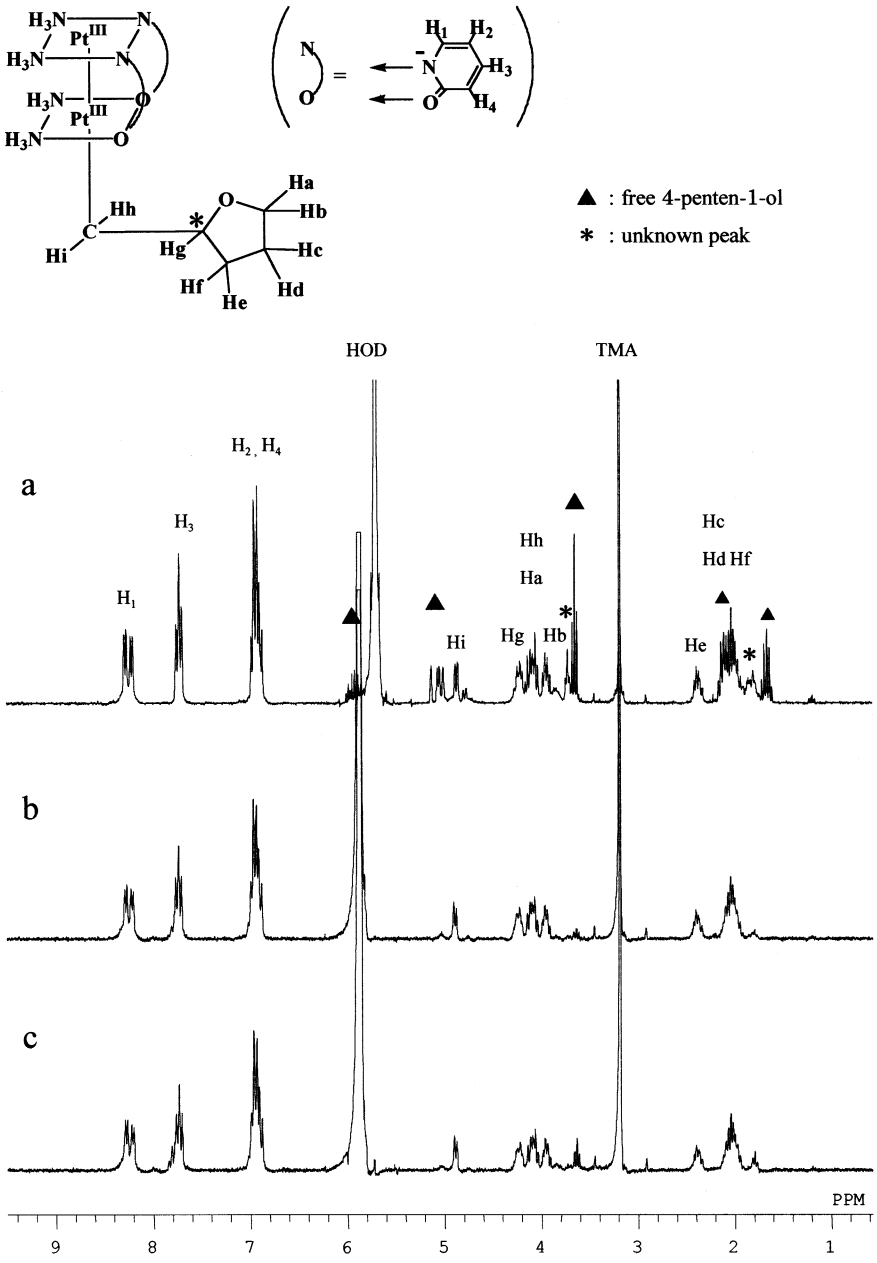

Figure 8. Change of the ^{1}H NMR spectrum with time at room temperature. $C_{HH} = 1.2 \times 10^{-2}$ M, $C_L = 2 \times 10^{-2}$ M, and $[DClO_4] = 1$ M. (a) At $t = 30$ min after mixing the HH dimer and the 4-penten-1-ol solutions. The reaction solution gave precipitate of the σ-complex after 30 min, and the following measurements [(b) and (c)] were done with the $DClO_4$ solution of once isolated precipitate of the σ-complex. (b) at $t = 45$ min and (c) at $t = 5$ h after the σ-complex precipitate was dissolved into 1 M $DClO_4$ (see text).

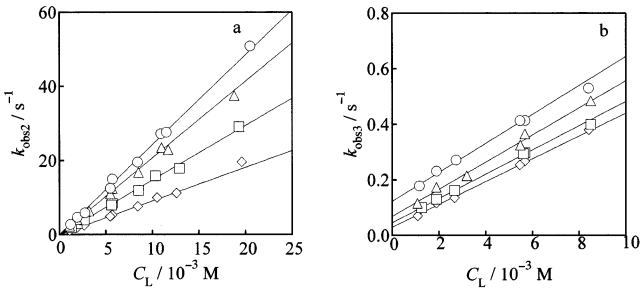

Figure 9. Dependence of the observed rate constants on C_L for the reaction with 4-penten-1-ol at $I = 2.0$ M and 25 °C. (a) For step 2, (b) for step 3. $[H^+]$/M = 0.0510 (○), 0.102 (△), 0.204 (□), and 0.408 (◇).

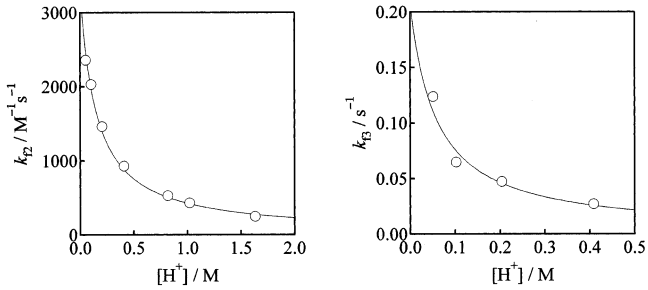

Figure 10. Dependence of k_{f2} ($= k_2 + k_2^{\#}K_{h2}/[H^+]$, slopes in Figure 9a) and k_{f3} ($= k_3K_{h3}/[H^+]$, intercepts in Figure 9b) on $[H^+]$ for the reaction with 4-penten-1-ol.

Pt^{II} complex are easily discernible from those of the Pt^{III} complex (see Figure 6)]. From these facts, the unknown product(s) seems to be still Pt^{III} alkyl complex(es) and is not released via reductive elimination.

The substitution reaction on the Pt^{III} dinuclear complexes usually proceeds consecutively, i.e., the first substitution occurs to the $Pt(N_2O_2)$ and the secondary to the $Pt(N_4)$ of the head-to-head complexes.[18] Even for the head-to-tail complex having two equivalent Pt(III) atoms, the reaction is consecutive.[19] If the faster step for the 4-penten-1-ol system corresponds to step 1 in the *p*-styrenesulfonate system, the plot of $(1 + K_{h1}/[H^+])$-k_{f1} vs $1/[H^+]$ must be linear according to eq 4. The result showed that this is not the case. The kinetic measurement was also performed at lower temperature (15 °C) and higher $[H^+]$. Under these conditions, step 1 in the *p*-styrenesulfonate system becomes slower, but the faster step in the 4-penten-1-ol system was not resolved into two steps. It seems that the step corresponding to step 1 in the *p*-styrenesulfonate system is still too fast to detect. Consequently, the observed faster step and the slower step were assigned to steps 2 and 3 in the *p*-styrenesulfonate system, respectively. The observed rate constants k_{obs2} and k_{obs3} for the faster (step 2) and slower (step 3) steps in the 4-penten-1-ol system, increased linearly with increasing C_L, and the slopes of the plot of k_{obs2} vs C_L decreased with increasing $[H^+]$ (Figure 9). On the other hand, the slope of the plot of k_{obs3} vs C_L was constant, whereas the intercept decreased with increasing $[H^+]$ as shown in Figure 9. Thus, the reaction mechanism of the 4-penten-1-ol system is constructed as in Scheme 5 on the basis of Schemes 3 and 4. According to the mechanism in Scheme 5, k_{obs2} and k_{obs3} are expressed as eqs 14 and 15, respectively, under the conditions, $C_{HH} \ll C_L$ and $[H^+] = 0.05-1.6$ M.

The data in Figure 9 were successfully analyzed according to eqs 14 and 15 as

$$k_{obs2} = k_{f2}[L] = \frac{k_2[H^+] + k_2^{\#}K_{h2}}{[H^+] + K_{h2}}[L] \doteq \left(k_2 + \frac{k_2^{\#}K_{h2}}{[H^+]}\right)[L] \quad (14)$$

$$k_{obs3} = k_{f3} + k_{d3}[L] = \frac{k_3K_{h3}}{[H^+] + K_{h3}} + k_{-3}[L] \doteq \frac{k_3K_{h3}}{[H^+]} + k_{-3}[L] \quad (15)$$

shown in Figure 10. The rate constants in eqs 14 and 15 are given in Table 1.

At step 2 in Scheme 5, the π-coordinated ligand on the $Pt(N_2O_2)$ is converted to the σ-coordinated ligand via intramolecular cyclization with proton release. After the conversion, the π-coordinated ligand on the $Pt(N_4)$ is liberated. There seems no water ligand on the $Pt(N_4)$ of the tetrahydrofurfuryl complex even in aqueous solution. Similar structure is found in the corresponding di-pivalamidato-bridged complex, which has no ligand on the $Pt(N_4)$ in solid state as shown by X-ray crystallography.[2]

Reaction with 4-Pentyn-1-ol. The reaction gave 1,5-dihydroxy-2-pentanone as the final product (eq 16). Much the same

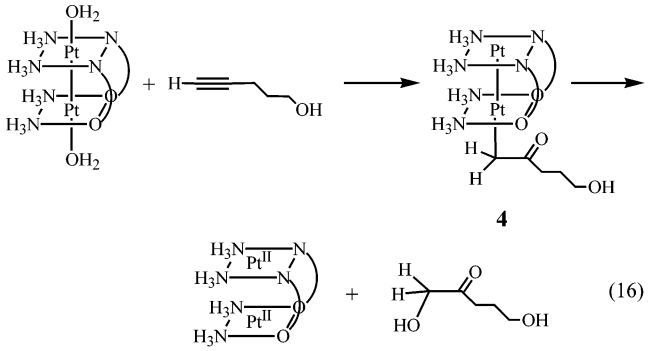

(16)

spectral change was observed for the reaction with 4-pentyn-1-ol (Figure SI-4). The dependence of k_{obs2} and k_{obs3} on C_L was also the same as for the 4-penten-1-ol system as shown in Figure 11. The ^{1}H NMR spectrum shows that the structure of the σ-complex **4** would be similar to that of the pivalamidato-bridged analogue $[(NH_3)_2Pt(\mu\text{-}((CH_3)_3CCONH)_2Pt(NH_3)_2(CH_2CO(CH_2)_3OH)]^{3+}$, whose structure was solved by X-ray crystallography.[26] Therefore, the reaction mechanism seems to be analogous to Scheme 5 and is shown in Scheme 6. The rate constants k_{obs2} and k_{obs3} are given by eqs 14 and 17, respectively. The analysis was reasonably performed as in Figure 12, and the obtained values are listed in Table 1

$$k_{obs3} = k_{f3} + k_{d3}[L] = \frac{k_3KK_{h3}}{[H^+] + K_{h3} + KK_{h3}} + k_{-3}[L] \quad (17)$$

Effect of the Axial Ligands on the Kinetics. The axial bond distances of some HH amidato-bridged dinuclear platinum(III) complexes are tabulated in Table 2. The $Pt(N_2O_2)$-carbon (X_1) distance does not change significantly among complexes **5**−**7**, whereas the Pt−Pt and the $Pt(N_4)$-X_2 distances become longer in the order: $-CH_2COCH_3 < -CH_2CHO < -CH_2\overline{CH(CH_2)_3O}$, as the electron density on the carbon atom (in X_1) ligated to the $Pt(N_2O_2)$ is higher, which is in accordance with the trans

(26) Lin, Y.-S.; Yamada, J.; Misawa, H.; Matsumoto, K. to be published elesewhere.

Scheme 5. Reaction Mechanism for the Reaction of the HH Dimer with 4-Penten-1-ol

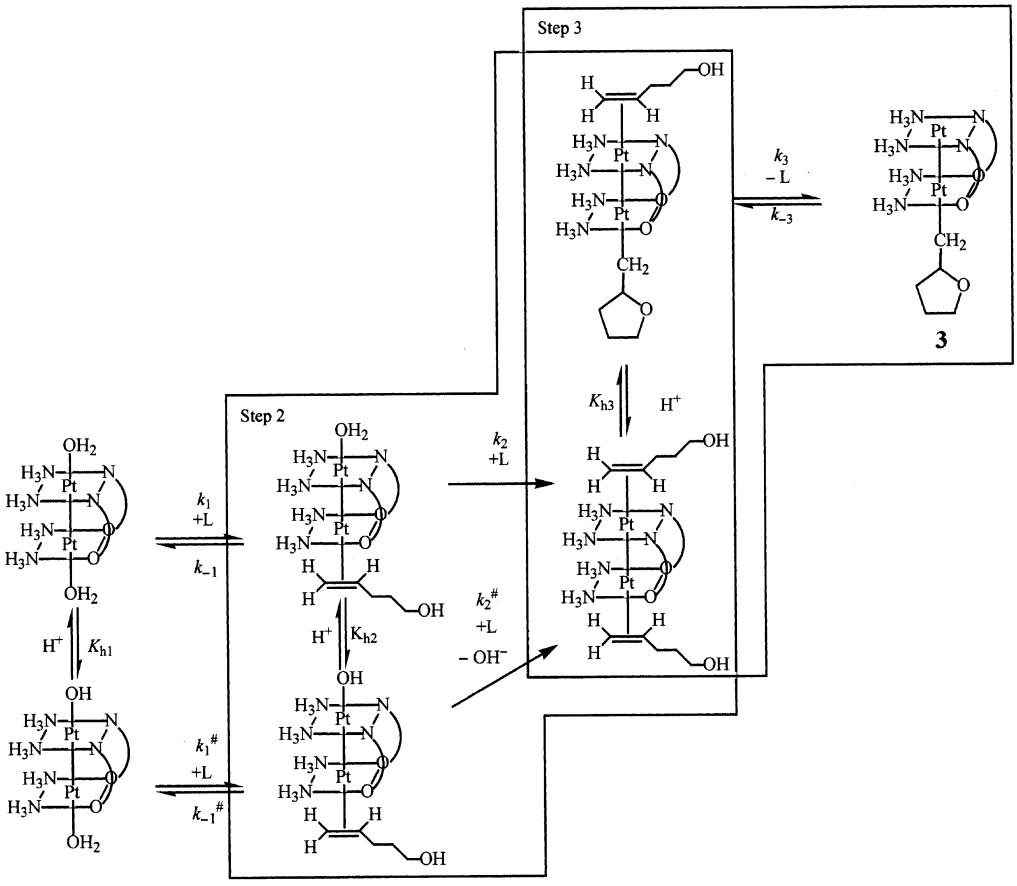

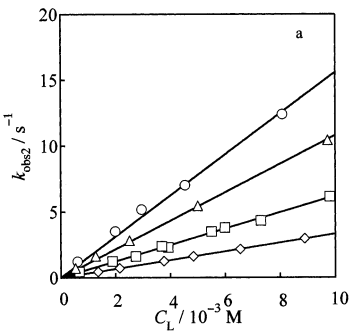

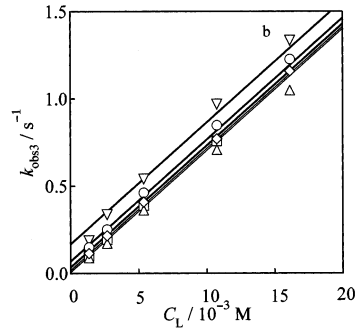

Figure 11. Dependence of the observed rate constants on C_L for the reaction with 4-pentyn-1-ol at $I = 2.0$ M and 25 °C. (a) For step 2, $[H^+]/M = 0.206$ (○), 0.411 (△), 0.805 (□), and 1.618 (◇); (b) for step 3. $[H^+]/M = 0.0411$ (▽), 0.103 (○), 0.206 (◇), 0.411 (□), and 1.23 (△).

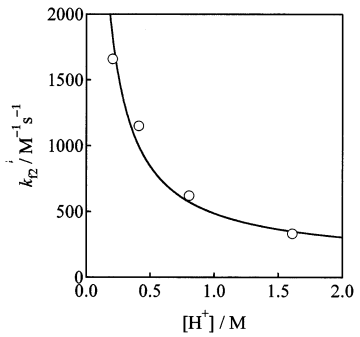

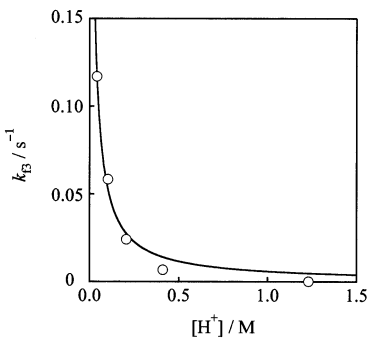

Figure 12. Dependence of k_{f2} ($= k_2 + k_2^{\#}K_{h2}/[H^+]$, slopes in Figure 11a) and k_{f3} ($= k_3KK_{h3}/([H^+] + K_{h3} + KK_{h3})$, intercepts in Figure 11b) on $[H^+]$ for the reaction with 4-pentyn-1-ol.

influence order of these ligands. In other words, as the trans influence of X_1 is stronger, the electron localization in the dinuclear complex $X_1-Pt^{IV}(N_2O_2)-Pt^{II}(N_4)-X_2$ becomes more prominent, i.e., the trans influence of X_1 appears on the other end of the Pt−Pt bond, and the $Pt(N_4)-X_2$ becomes longer. The order of trans influence in complexes **1**−**4** in Schemes 3−6, would be $-CH_2CH(OH)$-*p*-$C_6H_4SO_3^-$ < $-CH_2C(OH)(CH_3)$-$CHSO_3^-$, $-CH_2CO(CH_2)_2OH$, $-CH_2CH(CH_2)_3O$. The depen-

Scheme 6. Reaction Mechanism for the Reaction of the HH Dimer with 4-Pentn-1-ol

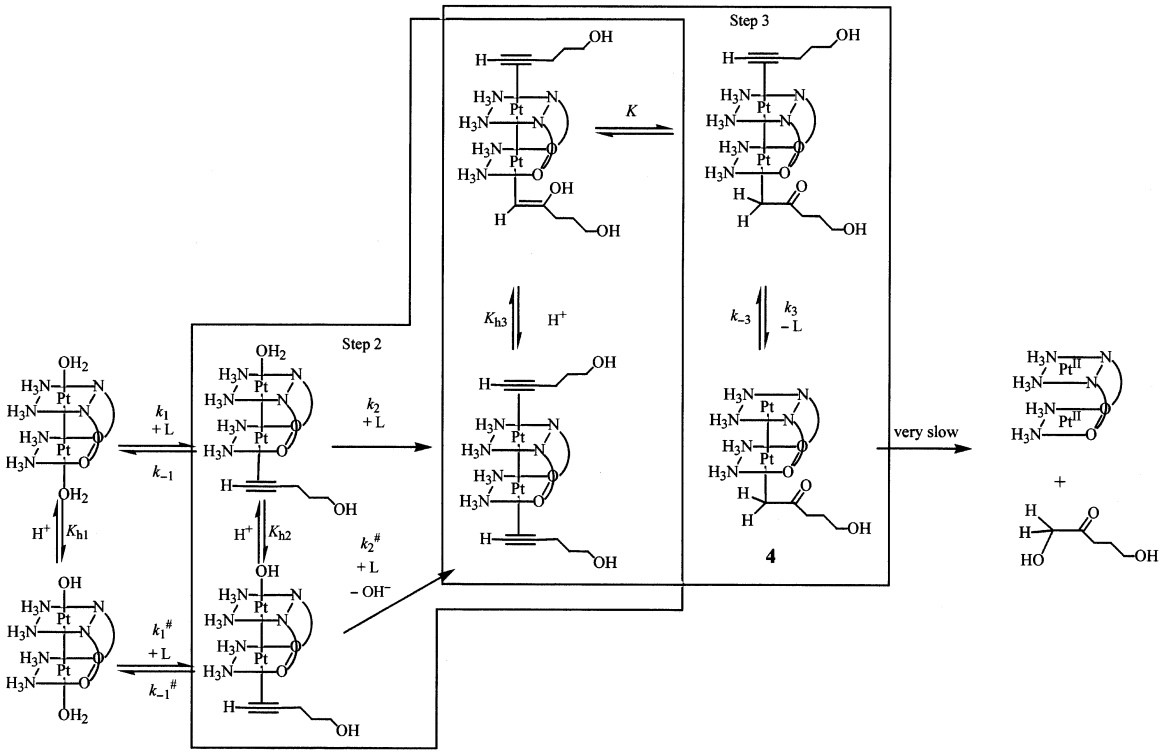

Table 2. Axial Bond Distances (Å) of the HH Amidato-Bridged *cis*-Diammineplatinum(III) Dinuclear Complexes

complex bridging ligand	5[a] pivalamidate	6[b] pivalamidate	7[b] pivalamidate	8[c] pivalamidate	9[c] pivalamidate	10[d] 2-pyrrolidonate	11[d] 2-pyrrolidonate
			$^{-}CH_2\overline{CH(CH_2)_3O}$				
X_1	$^{-}CH_2COCH_3$	$^{-}CH_2CHO$		$^{-}CH_2COC_6H_5$	$^{-}CH_2COCH_2COCH$	Cl^{-}	Cl^{-}
$Pt(N_2O_2)-X_1$	2.095(9)	2.121(9)	2.11(1)	2.15(2)	2.114(8)	2.360(4)	2.455(4)
Pt−Pt	2.6892(6)	2.7106(7)	2.7486(8)	2.676(1)	2.7206(6)	2.624(1)	2.6373(7)
$Pt(N_4)-X_2$	2.667(7)	2.7498(8)	2.92(1)	none	none	2.27(1)	2.392(4)
X_2	NO_3^{-}	NO_3^{-}	NO_3^{-}	none	none	NO_3^{-}	Cl^{-}

[a] ref 24. [b] ref 2. [c] ref 23. [d] ref 25.

dence of k_3 on C_L for step 3 in Scheme 3 (Figure 3c) indicating that H_2O is ligated on the $Pt(N_4)$ in complex **1** in aqueous solution is very much different from those of other systems in Schemes 4−6 (Figures 7b, 9b, and 11b). This fact suggests that there is no water molecule on the $Pt(N_4)$ in complexes **2**−**4** in aqueous solution. In fact, complex **7** having the ligand with the highest trans influence on the $Pt(N_2O_2)$, similar to complex **3**, has no substantial axial bonding at the $Pt(N_4)$ in solid.[24] The fact that only complex **1** has a water molecule on the $Pt(N_4)$ in aqueous solution can be explained as follows. Introduction of the electron-withdrawing group such as *p*-benzenesulfonate into the *σ*-coordinated alkyl group on the $Pt(N_2O_2)$ atom reduces the electron-localization in the dinuclear complex ($X_1-Pt^{IV}(N_2O_2)-Pt^{II}(N_4)-X_2$) to the less localized dimer having the electronic structure $X_1-Pt^{III}(N_2O_2)-Pt^{III}(N_4)-X_2$, and to facilitate water coordination to the $Pt(N_4)$ atom, whereas the coordination of the substituted alkyl group with more electron-donating property to the $Pt(N_2O_2)$ atom effects stronger trans influence, and invokes higher electron localization in the Pt−Pt bond, giving the structure $X_1-Pt^{IV}(N_2O_2)-Pt^{II}(N_4)-X_2$, and stabilizes the *σ*-coordinated alkyl complex. However, stabilization of the *σ*-coordinated alkyl complex is much influenced by the stability of the Pt−C bond to the nucleophilic attack. In fact, it was confirmed by ^1H NMR spectrometry that the acetonyl complex of the HH α-pyridonato-bridged Pt^{III} dinuclear complex is much more stable than the complexes **1**−**4**.

Step 2 in Schemes 4 and 5 has two paths, k_2 and k_3; in the k_2 path, direct substitution of the H_2O on the $Pt(N_4)$ with an olefin takes place, whereas the k_3 path involves a coordinatively unsaturated intermediate formed by the dissociation of H_2O on the $Pt(N_4)$. In contrast, step 2 in Schemes 5 and 6 has two paths, k_2 and $k_2^{\#}$, in which OH^{-} on the $Pt(N_4)$ is replaced by olefin. These difference among Schemes 3 − 6 can be explained by the properties of the *π*-coordinated olefins on the $Pt(N_2O_2)$. The double bond character of *p*-styrenesulfonate and 2-methyl-2-propene-1-sulfonate would be reduced, compared with other olefins, by the electron-withdrawing benzenesulfonate and sulfonate groups, respectively. As a result, the *π*-bonds between the $Pt(N_2O_2)$ and the olefins for *π*-styrenesulfonate and 2-methyl-2-propene-1-sulfonate systems would be more effectively strengthened by accepting more electrons from the filled orbitals of the $Pt(N_2O_2)$ atom, which, contrary to the *σ*-complex mentioned above, enhances the electron-localization from the dinuclear complex ($X_1-Pt^{III}(N_2O_2)-Pt^{III}(N_4)-H_2O$) to the electronic structure $X_1-Pt^{IV}(N_2O_2)-Pt^{II}(N_4)-H_2O$, and reduces the acidity of the water molecule on the $Pt(N_4)$ atom. The water molecule on the $Pt(N_4)$ is therefore easily released. In fact, the

K_{h2} values in Table 1 decreases from 1.0×10^{-2} M for 4-pentyn-1-ol to 3.8×10^{-4} M for *p*-styrenesulfonate.

The axially coordinated OH^- on the $Pt(N_4)$ atom trans to the π-bonding olefin on the $Pt(N_2O_2)$ atom can be replaced by the olefin at step 2 for the reactions with 4-penten-1-ol and 4-pentyn-1-ol as shown in Schemes 5 and 6. This is unusual considering the standard substitution reactions on mononuclear octahedral metal complexes, however, such a substitution was also observed in the second step of the substitution reaction between the HT 2-pyridonato-bridged Pt^{III} dimer and Cl^-.[19] The comparison of the complexes 10 and 11 in Table 2 shows that the $Pt(N_2O_2)-X_1$ as well as the Pt−Pt distances depend on X_2 even for the same X_1 on the $Pt(N_2O_2)$. When NO_3^- on the $Pt(N_4)$ (**10**) is replaced by Cl^- (**11**) having stronger trans influence, the $Pt(N_2O_2)-Cl$ distance becomes longer, and probably the $Pt(N_4)-X_2$ distance also becomes slightly longer, which suggests that the $Pt(N_4)-OH$ distance is longer than the $Pt(N_4)-OH_2$ distance with the same X_1, in other words, the electron localization in the HH dimer is less in the hydroxo complex than the aqua complex ($X_1-Pt^{IV}(N_2O_2)-Pt^{II}(N_4)-OH_2$, $X_1-Pt^{III}(N_2O_2)-Pt^{III}(N_4)-OH$). It can also be expressed as the inert $Pt^{IV}(N_4)$ in the aqua complex becomes more labile $Pt^{III}(N_4)$ in the hydroxo complex. More generally, the $Pt(N_2O_2)-X_1$, the $Pt(N_4)-X_2$, and the Pt−Pt distances are very dependent on both X_1 and X_2. These would be the reason OH^- on the $Pt(N_4)$ atom is subjected to substitution for the 4-penten-1-ol and 4-pentyn-1-ol systems.

In contrast to the *p*-styrenesulfonate system, step 1 was not observed for the 4-penten-1-ol and 4-pentyn-1-ol systems, probably because step 1 is too fast to detect, whereas only the tail of the reaction curve was observed for the 2-methyl-2-propene-1-sulfonate system. These observations are explained by the degree of nucleophilicity of the olefins or by the steric hindrance of the olefins.

Conclusions

In the reactions of the HH 2-pyridonato-bridged *cis*-diammineplatinum(III) dinuclear complex with olefins in acidic aqueous solution, the first substitution with an olefin molecule occurs to the $Pt(N_2O_2)$ atom to produce the mono-π complex, and the second substitution occurs to the $Pt(N_4)$ atom to form di-π complex. These steps are followed by dissociation of the second olefin on the $Pt(N_4)$ atom and the conversion of the first π-bonding olefin to the σ-bonding alkyl ligand on the $Pt(N_2O_2)$ atom under the conditions $C_{HH} \ll C_L$. When the resultant σ-complex is less stable, the σ-complex is reduced to produce the corresponding Pt^{II} dinuclear complex and ketone. The reactivity of the axial site of the $Pt(N_4)$ is much influenced by the nature of the ligand on the opposite axial site, and vice versa. The stability of the σ-complex depends on the nature of the ligand (R) on the $Pt(N_2O_2)$; the more the ligand is electron withdrawing, the more the electron in the Pt^{III} dimer is localized to $R-Pt^{IV}(N_2O_2)-Pt^{II}(N_4)$, to form more stable σ-complex. However, the stability is much more influenced by the susceptibility of the σ-complex to nucleophilic attack as exemplified by the acetonyl complex.

Under the conditions $C_{HH} > C_L$, where no olefin can coordinate to the $Pt(N_4)$ atom, the σ-complex would be formed directly from the mono-π complex.

The amidato-bridged Pt^{III} dimer complex presents a rare opportunity to study the mechanism of the olefin coordination and the successive nucleophilic attack. These reaction steps are closely related to Wacker reaction, and in the latter reaction, the π to σ conversion is slow.[27] In contrast, the conversion is a rapid equilibrium process in the present reactions. With regard to the axial olefin π-coordination, Natile et al. reports novel olefin coordination to $PtCl_2$(dmphen) (dmphen = 2,9-dimethyl-1,10-phenanthroline) at the axial site to give the five coordinate Pt(η^2-olefin)Cl_2(dmphen).[15] The formation constants for the reactions with several olefins are in the order of 10^2 M^{-1} at 25 °C. The formation constant for the reaction of the present Pt^{III} dimer with *p*-styrenesulfonate in step 1 is calculated to be $k_1/k_{-1} = 10^3$ M^{-1}, which is 1 order of magnitude larger than that of the above Pt(II) monomer reaction. Although no corresponding rate constant is reported for $PtCl_2$(dmphen), the rate constants of the Pt^{III} dimer complex for the π to σ conversion by water attack must be considerably higher than for the Pt(II) complex. The rate constants of the amidato-bridged Pt^{III} dinuclear complex with olefins are comparable to those with halide ions (in the order of 10^3 M^{-1} s^{-1}),[18,19] and considerably higher than those of the ligand substitution on Pt(II) complexes (in the range of $10^0 - 10^{-3}$ M^{-1} s^{-1}).[28]

Acknowledgment. We thank 21COE "Practical Nano-Chemistry" from MEXT, Japan for the financial support.

Supporting Information Available: Numerical values of the observed k_{obs} under various conditions, and related figures. This material is available free of charge via the Internet at http://pubs.acs.org.

JA020953S

(27) Henry, P. M. *J. Am. Chem. Soc.* **1964**, *86*, 3246, and references therein.
(28) (a) Basolo, F.; Grey, H. B.; Pearson, R. G. *J. Am. Chem. Soc.* **1960**, *82*, 4200. (b) Belluco, U.; Ettore, U.; Basolo, F.; Pearson, R. G.; Turco, A. *Inorg. Chem.* **1966**, *5*, 591. (c) Paxson, J. R.; Martin, D. S., Jr. *Inorg. Chem.* **1971**, *10*, 1551. (d) Palmer, D. A.; Kelm, H. *Inorg. Chim. Acta* **1976**, *19*, 117.